



Modeling the Diffraction of Electromagnetic Waves over Underwater Objects; the Wiener-Hopf Integral Equation

Yajni Warnapala^{1*} and Cole Foster¹

¹Department of Mathematics, Roger Williams University, Bristol, RI USA.

Authors' contributions

This research was carried out in collaboration between both authors. Dr. Yajni Warnapala designed the theoretical framework for the study and provided the original code for the program used for numerical calculations, Cole Foster carried out the programming, testing and the numerical analysis and synthesized the final results of the project. Both authors were involved with the writing of the manuscript and the conclusions of the final project.

Article Information

DOI: 10.9734/JAMCS/2020/v35i430276

Editor(s):

- (1) Dr. Jacek Dziok, University of Rzeszow, Poland.
- (2) Dr. Zhenkun Huang, Jimei University, China.

Reviewers:

- (1) Rahul Parbat, Savitribai Phule Pune University, India.
- (2) Tahreer Safa'a Mansour, Institute of Laser Graduate Studies, Baghdad University, Iraq.
- (3) Anusha R, NMAM Institute of Technology, India
- (4) Asmahani Awang, Universiti Malaysia Sabah, Malaysia.
- (5) Oluwaseun I. Kolawole, University of Nigeria, Nsukka, Nigeria.

Complete Peer review History: <http://www.sdiarticle4.com/review-history/58323>

Received: 22 April 2020

Accepted: 28 June 2020

Published: 09 July 2020

Original Research Article

Abstract

This research, inspired by the loss of Malaysian Airline Flight 370, investigates the feasibility of obtaining good convergence results for a model of the interaction of electromagnetic waves over the surface of the Spherical Biconcave Disc. The Galerkin Method is used to numerically solve the Dirichlet and Neumann exterior boundary value problems for the Wiener-Hopf Integral Equation over the half-plane of the Spherical Biconcave Disc. This modeling accounts for the attenuation losses of the propagating electromagnetic wave as a result of absorption and scattering in lossy media with comparison to lossless propagation. The numerical results of this research finds good convergence for this model as well as limitations in the transmission of electromagnetic waves underwater.

*Corresponding author: E-mail: ywarnapala@rwu.edu;

Keywords: Wiener-Hopf; galerkin; neumann; dirichlet; attenuation; lossless; lossy; plane-wave; propagation.

1 Introduction

With ocean covering over 70% of our planet, it is not surprising that the objects which fall into its depths are rarely recovered. This study, inspired by the loss of Malaysian Airline Flight 370, aimed to provide the theoretical framework for understanding the interaction of propagating electromagnetic waves at the surface of underwater objects. The objective of this study was to find a numerical solution to the Dirichlet and Neumann boundary value problems for the Wiener-Hopf Integral Equation model through the use of the Galerkin Method. The mathematical modeling of this integral equation yielded the convergence results of the model over the surface of the Spherical Biconcave Disc. The parameters of this Spherical Biconcave Disc were carefully chosen to mimic the shape of the turbine used on a Boeing 777 Passenger Jet.

The Wiener-Hopf Integral Equation has many applications, some of which include radiative transfer, electromagnetics, and optical oceanography. The equation is a Fredholm Integral Equation of the Second Kind. There are multiple methods of solving these equations analytically, as *A First Course in Integral Equations* [1] describes. The Adomian Decomposition Method was used to find the analytical solution to the Wiener-Hopf Integral Equation Model shown in Equation (1.1). However, solving these integral equations analytically is time consuming, and can become difficult as the complexity of the incoming wave function increases. In place of analytical solutions, this research turns to numerical methods to approximate the integral equation. The Galerkin Method is an extremely accurate method of integral approximation using Gaussian Quadrature nodes. FORTRAN 77 was used to generate the Galerkin coefficients and approximate the integral equation. As with any iterative method, the accuracy of the method increases with additional iterations. In order to find an approximation close to the true solution of the integral equation, it was important to use as many Gaussian Quadrature nodes as possible.

The Wiener-Hopf Equation has been heavily used in radiative transfer scenarios, notably for Milne's Problem [2]. Additionally, the Wiener-Hopf Integral Equation has been popular in the modeling of the diffraction of plane waves [3]. In his paper titled *Asymptotic Analysis of a Line Source Diffraction by a Perfectly Conducting Half-Plane in a Bi-Isotropic Medium*, Hussian uses the Wiener-Hopf Integral Equation to model line source diffraction with plane waves. Hussian's paper also references the works of Asghar and Lakhtakia [4] that investigated the source-free analysis for the diffraction of plane wave propagation. Colton and Kress investigated the use of integral equations in scattering theory [5]. Taking refraction into consideration, Jiang and Georgakopoulos more recently studied the transition of electromagnetic waves from air to fresh water [6].

Section 1 considers the Wiener-Hopf Integral Equation as a model of the interaction of electromagnetic waves at the surface of the Spherical Biconcave Disc. This study uses a point source to propagate electromagnetic waves through sea water, considering the impact of attenuation on the electromagnetic wave. Section 2 considers the Galerkin Method as a computational approximation of the integral equation. Section 3 considers the convergence results calculated over varying distances from the underwater Spherical Biconcave Disc. These results were recorded for the two separate boundary conditions, Dirichlet and Neumann, in both lossless and lossy environments. The results of this numerical analysis, its limitations, and potential future directions of this research are discussed in the Conclusion.

1.1 The Wiener-Hopf integral equation

The Wiener-Hopf Integral Equation is a nonlinear, weakly-singular Fredholm integral equation of the second kind [7]. The mathematical model for this equation in an exterior domain is given in

Equation (1.1).

$$u(P) = f(P) - \lambda \int_a^b e^{-P+Q} u(Q) dQ \quad (1.1)$$

$u(P)$ is the solution of the equation determined by the boundary function, $f(P)$ is the function of the incoming electromagnetic wave, P is the point in space, λ is the wavelength of the electromagnetic wave, Q is the point on the Spherical Biconcave Disc, and $[a, b]$ are the bounds of integration. The convergence results of this study were determined by the difference between the left and right hand sides of Equation (1.1). The value of $u(P)$ is dependent on the exterior boundary condition. The right hand side contains the propagating wave equation, $f(P)$, and the integral. The bounds of $[0, r]$ are used for this exterior boundary value problem, where r is the radius of the Spherical Biconcave Disc. The integrand, e^{-P+Q} , is the kernel of the integral equation found with the help of the unpublished works of Alen Alexandrian in *On Compact Operators*. The difference between the left and right-hand sides yielded the convergence results of the model. This research investigated the feasibility of obtaining good convergence results for the Dirichlet and Neumann boundary conditions. For this research, convergence results below 10^{-5} were considered good, with lower values deemed better.

The boundary conditions determine the value of $u(P)$ in the left hand side of Equation (1.1). The Dirichlet Condition is a type of boundary condition that specifies the value that a solution needs to take along a boundary of the domain. In the context of this research, this boundary condition implies that all incoming waves are absorbed by the boundary of the Spherical Biconcave Disc. The Neumann boundary condition is another boundary condition typically used in differential equations. The two boundary conditions are given in Equation (1.2) [8].

$$\begin{aligned} u(P) &= f(P) \\ \frac{\partial}{\partial n} u(P) &= f(P) \end{aligned} \quad (1.2)$$

Considering an application of object detection, the Neumann boundary condition is more fitting for the study.

1.2 The Spherical Biconcave disc



Fig. 1. Comparison of the GE90-115BL Turbofan (shown in Fig. (1a)) [9] on the Boeing 777 Jet and the Spherical Biconcave Disc intended to mimic its shape. The Spherical Biconcave Disc in Fig. (1b) was taken under parameters $\rho = 1.963m$, $A = 0.05$, and $B = 0.78$.

The Spherical Biconcave Disc was generated in Maple 2018. In spherical coordinates, the shape is defined by the three parametric equations in Equation (1.3).

$$\begin{aligned} x &= \rho \cos(\theta) \sin(\vartheta) \\ z &= \rho \sin(\theta) \sin(\vartheta) \\ y &= \rho \cos(\theta) (A + B(x^2 + z^2)) \end{aligned} \quad (1.3)$$

In Equation (1.3), $0 < \theta < \pi$, $0 < \vartheta < 2\pi$, ρ is the radius, and A and B are parameters adjusted to manipulate the shape of the Spherical Biconcave Disc. The arrangement of the parametric equations allows for the disc to rotate symmetrically about its y-axis. The code describing this shape is written into FORTRAN 77, where it serves as the boundary over which the incoming wave interacts.

Malaysian Airline Flight 370 was a Boeing 777-200ER passenger jet which contained two wing-mounted GE90-115BL turbo fans. The parameters of the Spherical Biconcave Disc were manipulated to mimic the specifications from General Electric [10]. According to the specification sheet from General Electric, the maximum width of the turbine is 154.56 inches, or 3.925 meters. Considering this diameter of 3.925 meters, this research used a radius of $\rho = 1.963$ meters for the Spherical Biconcave Disc. The specification sheet [10] also notes the absolute length, from "fan spinner to nozzle centerbody", to be 286.67 inches, or 7.28 meters.

Looking at Fig. (1a), it is clear that the black nozzle extends past the smooth, white surface of the rest of the turbine. To apply Green's Theorem, this research had to consider a smooth, closed-bounded shape. For this reason, only the front portion of this jet was mimicked by the Spherical Biconcave Disc. Considering the length of 7.28 meters, an assumption was made that 60% of the length is made up of that smooth section, making the length of the Spherical Biconcave Disc 4.386 meters. Under parameters $\rho = 1.963m$, $A = 0.05$, and $B = 0.78$, the Spherical Biconcave Disc takes on the shape of a plane turbine, while satisfying the length of 4.4 meters. The alignment of the shape to revolve around the Y-axis allows the shape to be laying on its side, as a real plane turbine would most likely rest on the ocean floor. Figs (1a) and (1b) and show the similarity between the Spherical Biconcave Disc and GE-115BL Jet Engine.

1.3 Transverse Plane Wave Propagation

Electromagnetic waves are a complex phenomenon. There are many ways to model these waves, and Transverse Plane Wave Propagation is arguably one of the simplest. In transverse plane wave propagation, the electromagnetic waves have an electric and a magnetic component that are coupled with each other. In phasor form, these waves are represented in Equation ((1.4)) [11].

$$\begin{aligned} \mathbf{E}_x &= \hat{x}E_0e^{-jkz} \\ \mathbf{H}_y &= \hat{y}H_0e^{-jkz} \end{aligned} \quad (1.4)$$

\mathbf{E} is the Phasor form of the Electric Field, \mathbf{H} is the Phasor form of the Magnetic Field, E_0 is the initial intensity of the electric field, H_0 is the initial intensity of the magnetic field, and k is the propagation constant. The equations within (1.4) take value in the \hat{x} and \hat{y} directions, while the direction of propagation is taken in the \hat{z} direction. Fig. (2) is a visual representation of this model, showing the orthogonal characteristics of the Electric and Magnetic components traveling in the arbitrary \hat{z} direction.

In Transverse Plane Wave Propagation, the electric and magnetic fields in the waves are coupled, and their relationship is dependent on the intrinsic impedance of the medium in which the wave is propagating, characterized by $\eta = \frac{E_0}{H_0}$ [11]. The coupling of the two equations was beneficial in applying numerical methods onto these wave functions- numerical results approximated on one component would be linearly related to the other. For this research, only the Electric component of the wave was considered.

Applying the complex conjugate of Eulers Identity, $e^{-j\theta} = \cos(\theta) - j\sin(\theta)$, to Equation (1.4) brings the sinusoidal equivalence of the Electric Field equation. The propagation constant, k , is related to the wavelength, λ , of propagating wave through $k = \frac{2\pi}{\lambda}$. Substitution gives Equation (1.5).

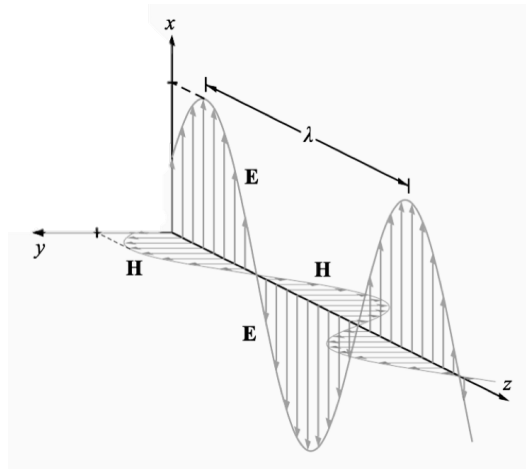


Fig. 2. Plane Wave Propagation, where the wave is propagating in the arbitrary \hat{z} direction. [11]

$$\mathbf{E}_x = \hat{x}E_0 \cos\left(\frac{2\pi}{\lambda}z\right) - j\hat{x}E_0 \sin\left(\frac{2\pi}{\lambda}z\right) \quad (1.5)$$

Equation (1.5) contains both a real and imaginary term. Since this research was focused in the real domain, the numerical methods can focus purely on the real term of the equation. Thus, this study only considered the first term in Equation (1.5).

1.3.1 Case 1: Propagation in Lossless Media

A lossless media is an ideal scenario where electromagnetic waves would not experience attenuation, such as in a vacuum. This study uses the baseline of a lossless medium to compare to the effects of attenuation in the lossy medium of seawater. In a lossless environment, the transverse plane wave propagation can be numerically analyzed with Equation (1.6).

$$\mathbf{E}(R) = E_0 \cos\left(\frac{2\pi}{\lambda}R\right) \quad (1.6)$$

In Equation (1.6), R is the distance the wave has traveled (replacing the arbitrary \hat{z} direction). This equation is an idealistic representation of Transverse Plane Wave Propagation. Realistically, the propagation of waves through any medium will result in attenuation losses.

1.3.2 Case 2: Propagation in Lossy Media

Equation (1.6) assumes a lossless medium, where the wave intensity would not decrease as a function of distance. Realistically, plane waves experience losses in intensity known as attenuation. In order to account for these losses, an exponential decay term, $e^{-\alpha R}$, was applied to this wave. The attenuation coefficient, α , helps define the total losses that the wave experiences while traveling through a lossy medium. This coefficient is dependent on the medium and the particular wavelength of the electromagnetic wave. Accounting for losses, the updated form of Equation (1.6) is shown in Equation (1.7).

$$\mathbf{E}(R) = E_0 e^{-\alpha z} \cos\left(\frac{2\pi}{\lambda}R\right) \quad (1.7)$$

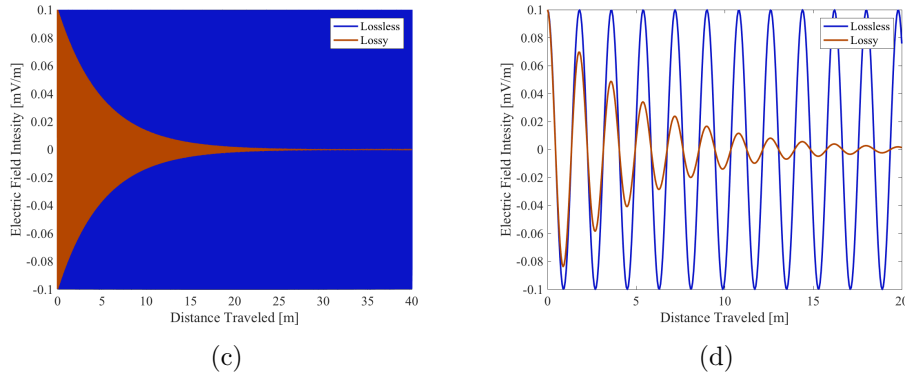


Fig. 3. Matlab generated plots of the transverse plane wave propagation functions used in lossless and lossy media used to show the characteristics of the waves. Fig. (3c) was generated with the true wavelength of 400 nm, while Fig. (3d) was generated with an arbitrary wavelength of 1.8 m to better show the sinusoidal nature of the waves

This research accounted for attenuation losses due to scattering and absorption, which are the inherent optical properties typically considered in attenuation [12]. The attenuation coefficient, α , is the sum of both α_a and α_s , the absorption and scattering coefficients. From C.D. Mobley's paper on *Radiative Transfer in the Ocean*, the values $\alpha_a = 0.029m^{-1}$ and $\alpha_s = 0.17m^{-1}$ for a wavelength $\lambda = 400nm$ were experimentally collected from samples of water in the North Atlantic Ocean [12]. Summed up, the attenuation coefficient for a wavelength of $\lambda = 400nm$ in salt water is $\alpha = 0.199m^{-1}$.

Both the lossless and lossy waves are showing in Fig. (3), where Fig. (3c) is the real nature of both the lossless and lossy waves, and Fig. (3d) better visualizes the sinusoidal nature by using a larger wavelength.

2 Numerical Methods

2.1 The Galerkin Method

The Wiener-Hopf Integral Equation is difficult to solve analytically. The Adomian Decomposition was used to prove convergence of the Equation under arbitrary parameters, but computational analysis techniques are able to produce approximations of the true solution. The Galerkin Method is an advanced analysis tool capable of providing extremely accurate approximations of integrals through the use of Gaussian Quadrature nodes. The Wiener-Hopf Integral is first transformed to a double integral, and then converted to the bounds of [-1,1].

This transformation is necessary because the Gaussian Quadrature method is based on an inner product of the Legendre Polynomials. In this research, Green's Theorem was used to convert the single integral to a double integral on the half-plane of the Spherical Biconcave Disc. The Galerkin Method was computed in the spherical coordinate system, which converts the approximation to what is shown below. The variable of integration is transformed to create a new integral equation on the unit sphere, which leads to the use of Spherical Harmonics, shown in Equation (2.1) as the basis function [13].

$$Y_n^m(\phi, \theta) = \left(\frac{m+1/2}{2\pi} \frac{(m-n)!}{(m+n)!}\right)^{1/2} p_n^m(\cos \theta) e^{im\phi} \tag{2.1}$$

In Equation (2.1), p_n^m is known as the Legendre Polynomials. This set of polynomials have the property in which any two of its polynomials are orthogonal to each other under an inner product. Another feature of these products is that their roots are within the interval [-1,1], which is why the integral must first be transformed to that interval. The Galerkin Coefficients, c_i , are also defined by using roots of the Legendre Polynomials. In spherical coordinates, the Wiener-Hopf Integral Equation can be approximated by the equivalence shown in Equation (2.2) [13].

$$\int_{-1}^1 \int_{-1}^1 f(t) dt \approx \frac{\pi}{M} \sum_{i=1}^{2M} \sum_{j=1}^M c_i Y(\phi_i, \theta_j) \tag{2.2}$$

In Equation (2.2), M is the number of intervals, c_i is the Galerkin Coefficients, $0 \leq \theta \leq 2\pi$, $0 \leq \phi \leq \pi$, and $Y(\phi_i, \theta_j)$ is the basis defined by Spherical Harmonics. For this research, a value of M=16 was used, beyond which further intervals did not seem to improve convergence. The function $Y(\phi_i, \theta_j)$ serves as the basis of the Galerkin method. FORTRAN 77 was used to computationally solve the Galerkin method of order n=5. The most recent results use an interval value of M=16, which gives an inner sum of 16 and an outer sum of 32. Further intervals increased computation time without providing better convergence results.

3 Results and Conclusions

3.1 Numerical Results

Convergence results for the Wiener-Hopf Integral Equation model were calculated at varying distances for different conditions. Earlier tests investigated the effects of changing the angle of propagation, but the results concluded that the angle did not influence convergence. The following results center around the Dirichlet and the Neumann boundary conditions. These conditions were tested for two cases, where the wave is propagating in lossy and lossless media.

Table 1. Table of Convergence Results for the Dirichlet and Neumann boundary conditions. All convergence results are on the order of E-05 or better, which was previously defined as good convergence. The convergence results were calculated for distances in powers of 2 for the purposes of logarithmic graphing as shown in Fig. 4.

Distance [m]	Lossless Conditions		Lossy Conditions	
	Dirichlet	Neumann	Dirichlet	Neumann
2	1.0800 E-06	1.0823 E-06	1.4082 E-05	1.9354 E-06
4	1.0800 E-06	1.0823 E-06	3.6135 E-05	6.3240 E-06
8	1.0800 E-06	1.0823 E-06	6.0896 E-05	1.1251 E-05
16	1.0800 E-06	1.0823 E-06	7.7106 E-05	1.4477 E-05
32	1.0800 E-06	1.0823 E-06	8.1076 E-05	1.5267 E-05
64	1.0800 E-06	1.0823 E-06	8.1248 E-05	1.5301 E-05
128	1.0800 E-06	1.0823 E-06	8.1248 E-05	1.5301 E-05
256	1.0800 E-06	1.0823 E-06	8.1248 E-05	1.5301 E-05
512	1.0800 E-06	1.0823 E-06	8.1248 E-05	1.5301 E-05
1024	1.0800 E-06	1.0823 E-06	8.1248 E-05	1.5301 E-05

3.1.1 Case 1: Propagation in Lossless Media

The lossless wave function for the Dirichlet condition, $E_1(R)$ is given by Equation (3.1), where an E_0 of 0.0001 V/m was used. For the Neumann condition, the normal derivative of Equation (3.1) was used.

$$E_1(R) = 0.0001 \cos\left(\frac{2\pi}{400 * 10^{-9}} R\right) \tag{3.1}$$

The numerical results for lossless conditions is summarized in Table (??), where convergence results are shown on an order of E-06, or 10^{-6} . It is noted that the convergence results do not change with distance, which is due to the lack of attenuation under lossless conditions. The Dirichlet Condition appears to have lower better convergence under lossless conditions. Table (??) shows that these convergence results were only slightly different, suggesting that the interaction of the electromagnetic waves over objects through lossless media does not vary much as the boundary conditions change.

3.1.2 Case 2: Propagation in Lossy Media

The lossy wave function for the Dirichlet Condition is given in Equation (3.2), where the exponential decay term is added. The normal derivative of Equation (3.2) is used for the Neumann Condition.

$$E_2(R) = 0.0001e^{-0.199R} \cos\left(\frac{2\pi}{400 * 10^{-9}} R\right) \tag{3.2}$$

The numerical results for lossy media are shown in Table (1) for both the Dirichlet and Neumann conditions. These results are on the order of E-05, or 10^{-5} . Figure (4) is a semi-logarithmic graph showcases the exponential pattern of the results for the two boundary conditions, where the convergence results eventually come to a plateau at 2^5 , or 32 meters. The Neumann condition appears to show better convergence under lossy conditions.

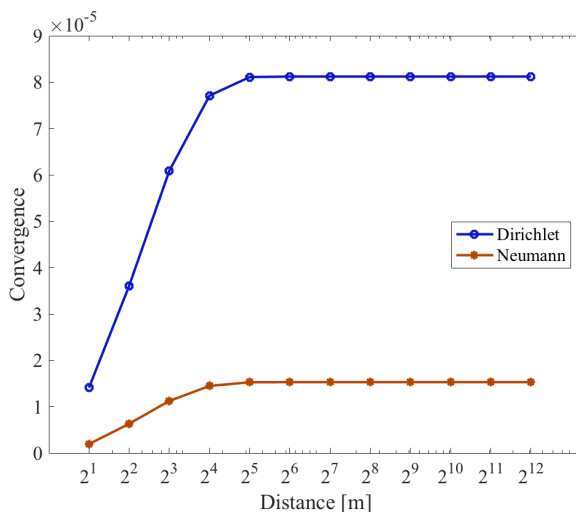


Fig. 4. Semi-logarithmic plot of the convergence results of the Wiener-Hopf Integral Equation Model for the propagation through lossy media

3.2 Conclusions

The convergence results in Section 3.1 suggest that the Wiener-Hopf Integral Equation model was successful in modeling the interaction of electromagnetic waves over the surface of the Spherical Biconcave Disc. The results for both boundary conditions with lossless and lossy media were all on the order of 10^{-5} , which was established as good convergence in Section 1.1. Fig. (4) shows the lossy electromagnetic waves had an exponential behavior as a result of the attenuation, where the convergence eventually leveled out at 2^5 , or 32 meters. In lossy conditions, the Neumann condition provided better convergence results than the Dirichlet condition under lossy conditions. One interesting behavior shown in this figure is the plateau effect after a distance of 32 meters. This is due to the attenuation losses of the propagating electromagnetic wave. As shown in Fig. (3c), attenuation impacts the power of a wave as it travels through a lossy media. These results show that the attenuation of electromagnetic waves in seawater is a limitation in transmission. In lossy conditions, the convergence results leveled out at 32 meters, whereas the average depth of the ocean is about 4000m.

This research required many assumptions to help focus its scope. For simplicity, this project assumed that the conditions of the ocean did not change with depth. It is well known that this is not the case, as temperature and pressure changes as the depth increases. These changes are gradual as the depth increases, but they may have a refractive effect on the propagating waves. Furthermore, this research uses attenuation coefficients from C.D. Mobley's paper on *Radiative Transfer in the Ocean* [12]. These coefficients were gathered from samples of water taken from the Atlantic Ocean rather than the Indian Ocean. The conditions of the Indian Ocean are different from the Atlantic- this includes differences in temperature and turbidity. These differences would impact the values of the scattering and the absorption coefficients. In future research, it would be better to treat the coefficients as functions of depth and turbidity. Additionally, this research project considered the two boundary conditions of the Dirichlet and Neumann condition. These two conditions assume that all incoming waves are absorbed or reflected, respectively. The Robin condition is a more realistic boundary condition which assumes that incoming waves are both absorbed and reflected. This research also simplified the plane wave propagation model to only include the real term of the wave. The inclusion of the imaginary term in future research would help better understand the phase of the wave as it propagates through the ocean.

Acknowledgements

We would like to thank Dr. Rutherford and Mrs. Kennedy for their technical support.

Competing Interests

Authors have declared that no competing interests exist.

References

- [1] Wazwaz, Abdul-Majid. A first course in integral equations. World Scientific; 2015.
- [2] Vanmassenhove FR. Exact analytical solution and numerical treatment of the milne problem with absorption and anisotropic scattering. *Physica*. 1968;42.
- [3] Hussain W. Asymptotic analysis of a line source Diffraction by a perfectly conducting half-plane in a Bi-isotropic medium. *Progress in Electromagnetic Research*. 2005;58.

- [4] Asghar S, Lakhtakia A. Plane-wave Diffraction by a perfectly conducting half-plane in a homogeneous bi-isotropic medium. *Int. J Appl. Electromagnetics in Materials*. 1994;5.
- [5] Colton D, Kress R. Integral equation methods in scattering theory. *Soc. Ind. Appl. Math.* 2013;6690.
- [6] Jiang Shan, George Akopoulos, Stavros. Electromagnetic wave propagation into fresh water. *Journal of Electromagnetic Analysis and Application*. 2011;3.
- [7] Atkinson KE. The numerical solution of the laplaces equation in three dimensions. *SIAM J. Numer. Anal.* 1982;19:263274.
- [8] Simscale. What Are Boundary Conditions?
(Accessed 20 May 2020)
Available:<https://www.simscale.com/docs/simwiki/numerics-background/what-are-boundary-conditions/>
- [9] General electric. GE90 Commercial Aircraft Engine.
Available: <https://www.geaviation.com/commercial/engines/ge90-engine>
- [10] General electric company. Type-certificate data sheet for GE90 series engines. European Union Aviation Safety Agency; 2019.
- [11] Ulaby Fawwaz, Ravaioli Umberto. *Fundamentals of applied electromagnetics*. Pearson Education; 2015.
- [12] Mobley CD. *Radiative transfer in the ocean*. Addison-Wesley Professional; 2001.
- [13] Lin Chu-Tzu, Warnapala Yajni. The numerical solution of exterior neumann problem for helmholtzs equation via modified greens functions approach. *Computers Mathematics with Applications*. 2004;47.

© 2020 Warnapala and Foster; This is an Open Access article distributed under the terms of the Creative Commons Attribution License (<http://creativecommons.org/licenses/by/4.0>), which permits unrestricted use, distribution and reproduction in any medium, provided the original work is properly cited.

Peer-review history:

The peer review history for this paper can be accessed here (Please copy paste the total link in your browser address bar)

<http://www.sdiarticle4.com/review-history/58323>